Available online at www.sciencedirect.com
ScienceDirect
Ceramics International 37 (2011) 891–896
CERAMICS INTERNATIONAL
www.elsevier.com/locate/ceramint

Preparation and properties of 2D C/SiC–ZrB_2–TaC composites

Lulu Li, Yiguang Wang *, Laifei Cheng, Litong Zhang

National Key Laboratory of Thermostructure Composite Materials, Northwestern Polytechnical University, Xi'an, Shaanxi 710072, PR China

Received 30 August 2010; received in revised form 8 September 2010; accepted 27 October 2010
Available online 3 December 2010

Abstract

Two-dimensional (2D) C/SiC–ZrB_2–TaC composites were fabricated by chemical vapor infiltration (CVI) combined with slurry paste (SP) method. 2D laminate was prepared by stacking carbon cloth that was pasted with a mixture of polycarbosilane–ZrB_2–TaC slurry. A small amount of carbon fiber tows were introduced into the preform in the vertical direction. After heat-treated at 1800 °C, the 2D laminate was densified with SiC by CVI to obtain 2D C/SiC–ZrB_2–TaC composites. Properties including flexural strength, interlaminar shear strength, and thermal expansion of the composites were investigated. The ablation test was carried out under an oxyacetylene torch flame. The morphologies of the ablated specimens were analyzed. The results indicate that the adding vertical fiber tows and heat-treatment at 1800 °C can greatly improve the mechanical properties of the composites. The co-addition of TaC and ZrB_2 powders into C/SiC composite effectively enhance its ablation resistance.

Keywords: C. Mechanical properties; Ceramic matrix composites; Ablation properties; Chemical vapor deposition

1. Introduction

Carbon fiber reinforced silicon carbide (C/SiC) composites have many excellent properties such as low density, high thermal conductivity, good thermal shock tolerability, and excellent high-temperature strength. Particularly, C/SiC composites show excellent oxidation and ablation resistance at temperatures below 1700 °C due to the formation of protective silica layer [1–4]. These excellent properties render them as potential materials for applications in aircraft and aerospace filed as engines, nose caps, leading edges, nozzles, and thermal protection systems for reusable space vehicles [5,6]. However, advanced space vehicles that will fly at hypersonic speed require the materials capable of prolonged operation in oxidizing atmosphere above 2000 °C [7]. C/SiC composites cannot meet the requirements because the protecting silica layer becomes active at such high temperatures, leading to the rapid ablation at the scouring of the ultrahigh temperatures and high pressure flux. It is necessary to improve their ablation resistance at ultrahigh temperatures.

Many efforts have been made to improve the ablation resistance of C/SiC composites either by creating ablation-resistant matrix or by applying ablation-resistant coatings [8–10]. Although ultrahigh-temperature coatings can enhance the ablation resistance of composites in short term, the ablation-resistant matrix is required for the prolonged operation at ultrahigh temperatures. Introducing refractory carbide/boride compounds into C/SiC composites is one of the widely used methods to improve the ablation resistance of the matrix. The refractory carbide/boride compound such as ZrB_2 or TaC was introduced into C/SiC matrix by slurry infiltration (SI) or by fiber-powder molding technique [11–17]. The content of the refractory compounds introduced by these methods is so limited that the ablation resistance of C/SiC composites cannot be obviously improved. A new method of slurry paste (SP) combined with CVI has been developed to introduce ZrB_2 into C/SiC composites. The ablation resistance of the obtained C/SiC–ZrB_2 was enhanced [18]. ZrB_2 was oxidized to ZrO_2 at ablation environments. Although ZrO_2 has a very high melting point (2715 °C), it is easily blown off the substrate under high-speed air scouring in the ablated area. The carbon fibers become uncovered, leading to acceleration in ablation.

In order to further improve the ablation resistance of C/SiC–ZrB_2 composites, TaC was added to the ZrB_2–SiC matrix. Under oxidizing environments, TaC can be oxidized to Ta_2O_5 oxide, which has a melting point of 1870 °C. At ablation temperature higher than 2000 °C, Ta_2O_5 melt is expected to bond ZrO_2, to seal the cracks, and to protect the fibers inside. In

* Corresponding author. Tel.: +86 29 88494914; fax: +86 29 884920.
E-mail address: wangyiguang@nwpu.edu.cn (Y. Wang).

0272-8842/$36.00
doi:10.1016/j.ceramint.2010.10.033

this paper, 2D C/SiC–ZrB_2–TaC composites were fabricated by SP combined CVI method. The ablation behavior of the obtained composites was tested. The results showed the increase in the ablation resistance by the addition of TaC in the matrix.

2. Experimental process

2.1. Composite preparation

The T-300^{TM} plain woven carbon cloth (fiber volume fraction ~40%, HTA-1000, TOHO, Japan) was cut into 100 mm × 100 mm pieces. A thin pyrocarbon layer was deposited on the fiber cloth by chemical vapor deposition at 960 °C using propane (C_3H_6) as precursor, followed by graphitization treatment at 1800 °C in argon atmosphere to obtain a weak interphase. TaC powder (Fernandez size 0.91 μm, Ningxia Orient Tantalum Industry Co., Ltd., Ningxia, China), ZrB_2 powder (particle size ~0.5 μm, Beijing Mountain Technical Development Center for Non-Ferrous Metals, Beijing, China), and liquid polycarbosilane (LPCS, Laboratory of Advanced Materials at Xiamen University, Xiamen, China) with a mass ratio of 1:1:4 were sufficiently mixed, and then pasted uniformly on each sheet. These sheets were stacked along the directions of woven cloth. A small amount of carbon fiber tows were introduced into the 2D laminate along the vertical direction. Subsequently, the preform with the slurry was thermal cured at 170 °C for 6 h under a pressure of 0.2 kPa, followed by pyrolysis at 900 °C for 4 h and heat-treatment at 1800 °C for 2 h. After that, CVI was used to introduce the SiC into the composites. The infiltration process was carried out at 1000 °C using methyltrichlorosilane (MTS, CH_3SiCl_3) as precursor. The as-fabricated composites were machined to the desired shapes for mechanical and ablation tests.

2.2. Tests and characterization

The flexural strength was measured using a three-point bending test (SANS CMT 4304, Sans Testing Machine, Shen Zhen, China) with a span of 30 mm. At least three samples with a dimension of 40 mm × 5 mm × 3.5 mm were used for the test. The loading rate was 0.5 mm/min, and the loading direction was parallel to the stacking direction of 2D C/SiC–ZrB_2–TaC. The force–displacement curves were recorded by computer. The interlaminar shear strength (ILSS) was measured by double-notched shear (DNS) method according to the standard of ASTM C1425-05. At least three samples with double notches were used in the test. The distance between two notches was 6 mm, and the depth of each notch was one half of the specimen thickness. The ablation tests were carried out in a vertically jetted flowing oxyacetylene torch environment. The exposure time under the torch flame was 20 s. At least three samples with a dimension of Φ30 mm × 5 mm were used in the test. Further detail about the test process was described elsewhere [10]. The temperature distribution on the sample surface was calculated using the FLUENT software based on the method of Gibbs free energy minimization. It was assumed that there was no friction between the flowing gas and equipment tube. The results showed that the heat flux was about 4200 kW/m^2 (±10% error) and the temperature in the center of the sample was about 3000 °C, which was in accordance with the measured temperature by the multiwavelength pyrometer [19].

The coefficient of thermal expansion (CTE) of the sample was measured by thermal dilatometer (DIL 402 C, Netzsch, Selb, Germany). The testing temperatures ranged from room temperature to 1350 °C. The ramping rate was 3 K/min and high-purity argon was used as protecting gas with a velocity of 50 ml/min. The phases of composites were analyzed by X-ray diffraction (XRD, Rigaku D/max-2400, Tokyo, Japan) with Cu K_α radiation. Data were digitally recorded in a continuous scan mode in the angle (2θ) range of 10–80° with a scanning rate of 0.12°/s. The microstructures of the specimens were observed by scanning electron microscope (SEM, JEOL 6700F, Tokyo, Japan) and the elemental analysis was conducted by energy dispersive spectroscopy (EDS). The density of the samples was measured by the Archimedes method with distilled water.

3. Results and discussion

The cross-section of the C/SiC–ZrB_2–TaC composites is shown in Fig. 1. It can be seen that the areas between the fiber bundles (Fig. 1a) are filled by the slurry as well as the fiber tows

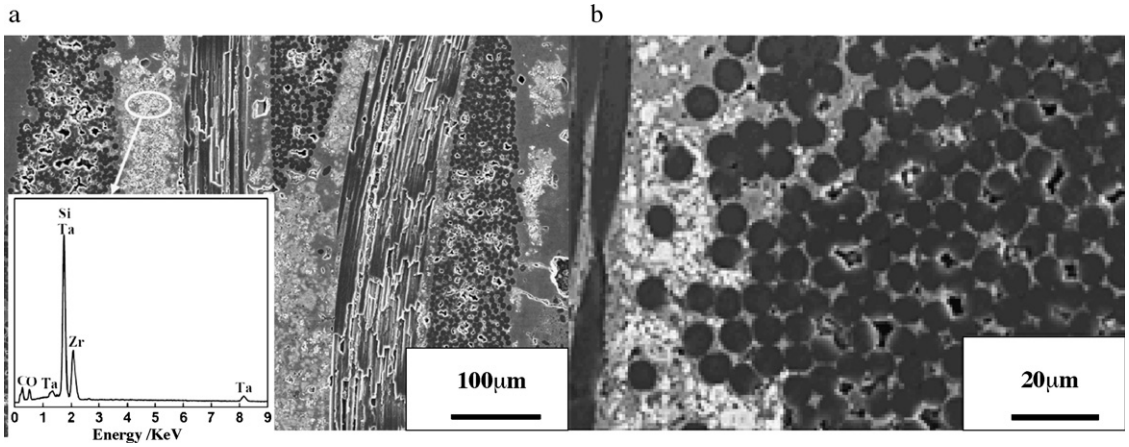

Fig. 1. (a) Cross section of 2D C/ZrB_2–SiC–TaC with EDS analysis; (b) 2000× partial enlarged pattern of (a).

inside (Fig. 1b). There are seldom large pores existing in the matrix. Only a mount of small pores in the fiber bundles could be found. During pyrolysis of the polymer precursor at high temperatures, a large number of volatile gases evaporate out [20]. The evaporation will produce the diffusion channels for further CVI SiC to densify the composites. A relatively dense composite can be obtained. EDS analysis (Fig. 1a) shows that the filled substances in the inter-bundle areas have a composition of B, C, O, Si, Ta, and Zr. It is believed that the substances are composed of ZrB_2, TaC, ZrO_2, Ta_2O_5, and SiC. ZrB_2 and TaC are the fillers. ZrO_2 and Ta_2O_5 are impurities on the surfaces of the fillers. SiC is deposited by CVI process, which will fill the pores or channels between the fibers and in the fillers.

A typical flexural strength–deflection curve of C/SiC–ZrB_2–TaC composites is shown in Fig. 2a. As comparison, the strength–deflection curve of C/SiC–ZrB_2 composites is also shown in Fig. 2a [18]. The flexural strength of C/SiC–ZrB_2–TaC is calculated to be 255 ± 15 MPa. The fracture behavior of the composites shows a typical pseudo-plastic deformation. There is no catastrophic failure behavior, which is attributed to the fiber pull-out during the deformation process (Fig. 2b). Compared with our previous research on C/SiC–ZrB_2 [18], both the strength and the ductility of C/SiC–ZrB_2–TaC are enhanced. The heat-treatment of the composites at 1800 °C is the reason. At 1800 °C, LPCS can promote the sinterability of ZrB_2–TaC powders by removal of the oxide scales on the starting powders and by the formation of volatile silicon at high temperatures [21], which will benefit for the strength of the matrix. Despite the heat-treatment at 1800 °C, the fibers are well protected during slurry paste, heat-treatment, and CVI process (Fig. 2c).

The interlaminar shear strength of C/SiC–ZrB_2–TaC composite is calculated to be 27.4 ± 5.1 MPa. The value is about twice of the interlaminar shear strength of the C/ZrB_2–SiC composite that is puncture-free along the vertical direction [18]. As shown in Fig. 3a, the shear failure occurs along the plane between the ends of the two notches. The shear surface goes through the SiC–ZrB_2–TaC matrix and along the interface between the carbon sheets (Fig. 3b). It is believed that the addition of vertical fiber tows and heat-treatment at 1800 °C are the reasons for high interlaminar shear strength of C/SiC–ZrB_2–TaC. As aforementioned, the heat-treatment at 1800 °C will increase in the strength of the SiC–ZrB_2–TaC matrix. The vertical fiber tows can enhance the connection between the carbon sheets. The interlaminar shear strength of the composites is thus obviously improved.

The CTE of C/SiC–ZrB_2–TaC is measured to be 3.2×10^{-6}/K. It is close to the value of 2D C/SiC (3.0×10^{-6}/K) [22], which was fabricated by the same CVI process as C/SiC–ZrB_2–TaC. It indicates that the adding refractory carbide powders into the C/SiC composites do not obviously affect on their thermal expansion properties. However, the calculated CTE of C/SiC–ZrB_2–TaC is about 3.7×10^{-6}/K according to the mixture rule, higher than the value of 3.2×10^{-6}/K. It is believed that the interface of the composites should determine the CTE of the composites. As shown in Fig. 1, the SiC is uniformly deposited on the pyrolytic carbon coated carbon fibers. The basic interface is still carbon fiber/pyrolytic carbon/SiC, similar to 2D C/SiC composites. The CTE of C/SiC–ZrB_2–TaC is thus same as that of C/SiC composites. Similar phenomena were also observed in other studies [23,24].

The ablation properties of C/SiC–ZrB_2–TaC composites were tested by exposure of the composites to an oxyacetylene

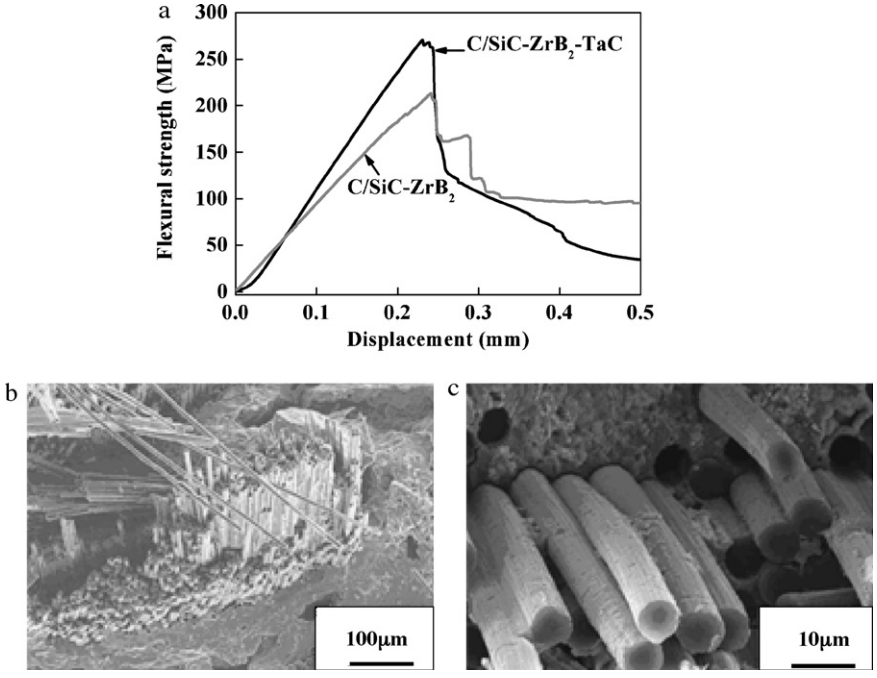

Fig. 2. (a) Typical strength–displacement curves of fracture of C/SiC–ZrB_2–TaC composite and C/SiC–ZrB_2 [18]; (b) flexure fracture surface of 2D C/SiC–ZrB_2–TaC composite; (c) 2000× partial enlarged fracture surface.

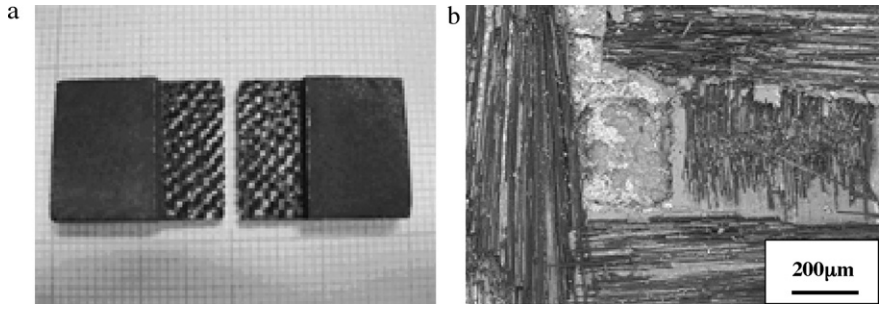

Fig. 3. Morphologies of the interlaminar shear fracture of 2D C/SiC–ZrB_2–TaC: (a) macro photograph; (b) interlaminar shear fracture surface.

Table 1
The linear ablation rates of C/SiC, C/SiC–ZrB_2, C/SiC–TaC and C/ SiC–ZrB_2–TaC.

Sample	Line-ablation rate (mm/s)	Density (g/cm^3)	Open porosity (%)
C/SiC [8]	0.083	2.37	10
2D C/ZrB_2–SiC [18]	0.066	2.10	–
2D C/SiC–TaC [8]	0.038	3.03	13
2D C/SiC–ZrB_2–TaC	0.026	2.35	11.5

torch flame for 20 s. The linear ablation rate of the C/SiC–ZrB_2–TaC is listed in Table 1. The linear ablation rate was calculated by the eroded depth at the ablation center dividing the ablation time. As comparison, the linear ablation rates of C/SiC, C/SiC–ZrB_2, and C/SiC–TaC are also listed in Table 1. As can be seen, co-addition of ZrB_2 and TaC can greatly increase the ablation resistance of C/SiC composites.

As shown in Fig. 4b, the composites are well protected after ablation, and no large-scaled bareness or erosion of fibers can be found. There are three obvious regions on the surface of the

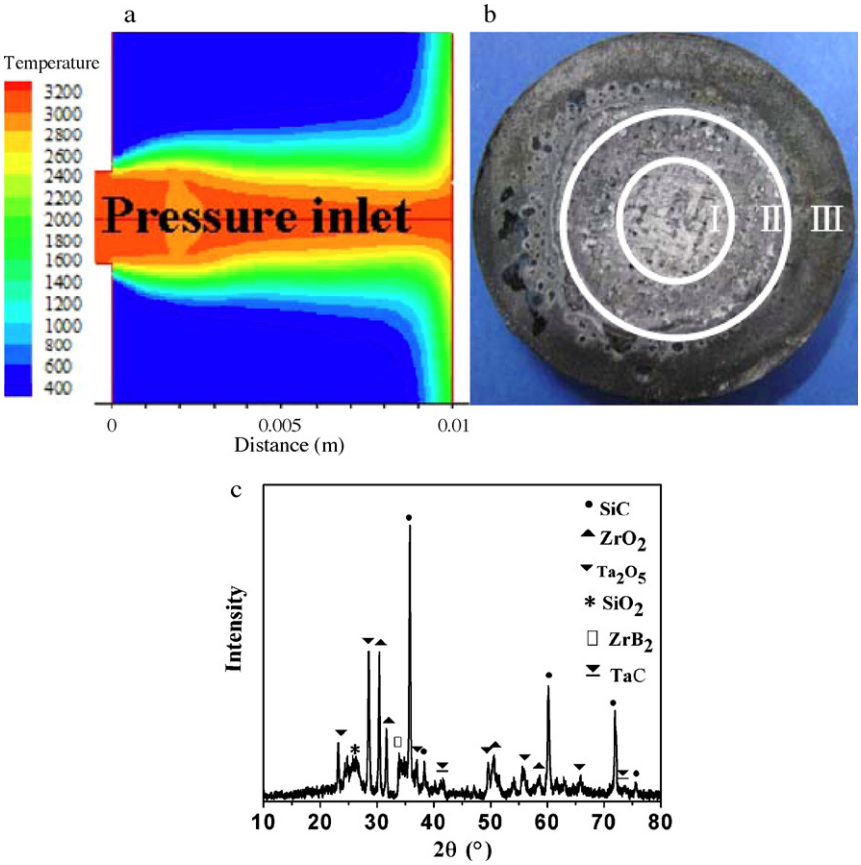

Fig. 4. (a) Simulation for the temperature distribution of the ablation sample by FLUENT software; (b) macro photograph of the sample after ablation (c) XRD pattern of 2D C/ZrB_2–SiC–TaC composite after ablation for 20 s.

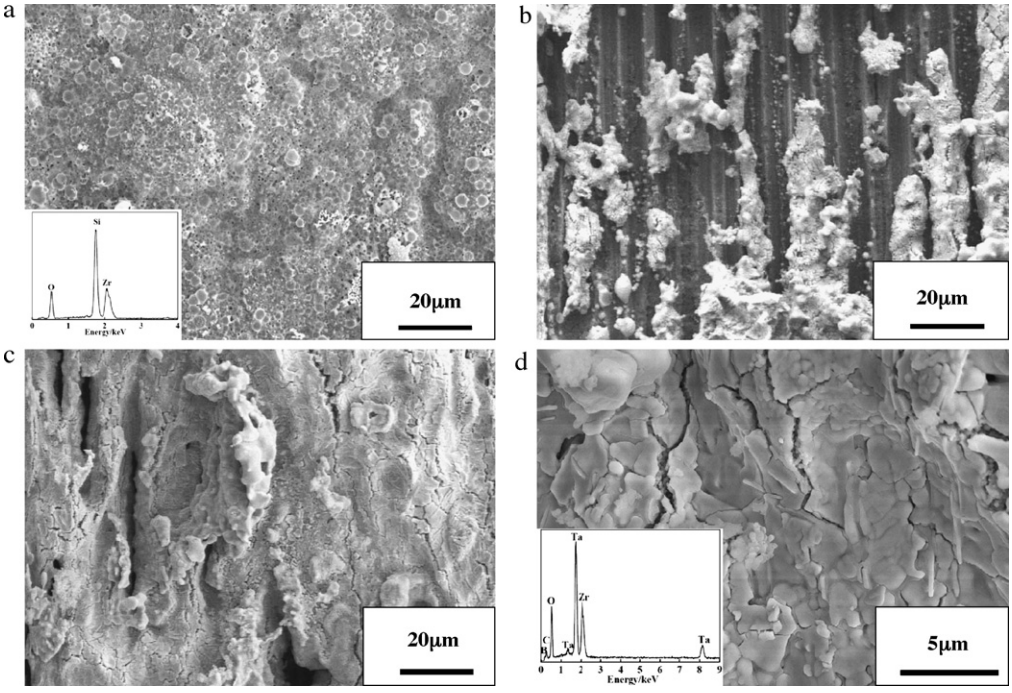

Fig. 5. Morphologies of the samples after ablation: (a) the morphology of the ablated area at the border between region II and region III; (b) nude fibers in ablation central; (c) dense oxide coating in ablation center; (d) 5000× partial enlarged morphology of the dense coating at ablation center.

tested sample: the ablation center (region I) that was seriously ablated; the transition region (region II); and the ablation fringe (region III) that was slightly eroded. As indicated by the calculated results (Fig. 4a), the temperature at the center of ablated sample is about 3000 °C, while the temperatures in region III are less than 1800 °C. XRD result (Fig. 4c) indicates that the oxides on the ablated surface are mainly Ta_2O_5, ZrO_2, and SiO_2. It is believed that the following reactions would happen during the ablation process:

$$SiC(s) + O_2(g) \rightarrow SiO_2(l) + CO(g) \quad (1)$$

$$SiC(s) + O_2(g) \rightarrow SiO(g) + CO(g) \quad (2)$$

$$SiO_2(l) + CO(g) \rightarrow SiO(g) + CO_2(g) \quad (3)$$

$$ZrB_2(s) + O_2(g) \rightarrow ZrO_2(l) + B_2O_3(g) \quad (4)$$

$$4TaC(s) + 7O_2(g) \rightarrow 2Ta_2O_5(s,l) + 4CO(g) \quad (5)$$

The morphology of the area at the border between region II and region III is shown in Fig. 5a. It can be seen that there are glass phases with some bubbles and pores in this area. The EDS analysis indicates that the glass phases are silica combined with zirconia. The layer of the mixture of silica and zirconia can prevent the samples from being further ablated. As indicated by Fig. 4a, the temperatures close to region II are higher than 1800 °C, at which the oxidation of SiC becomes active according to reactions (2) and (3). The volatilization of SiO and B_2O_3 (according to reaction (4)) results in the bubbles in Fig. 5a. As the temperature becomes higher, the evaporation of SiO becomes more seriously so that there is less silica visible close to the ablation center.

At the ablation center (region I), there are two kinds of morphologies: one is the uncovered fibers with a few oxides on them (Fig. 5b), and the other is the fibers with a compact oxide layer covered (Fig. 5c). As indicated by EDS analysis, the main phases of the dense layer and the substances on the uncovered fibers are Ta_2O_5 and ZrO_2. The different morphologies in the ablation center are caused by the small content of TaC in the matrix and the uneven distribution of the TaC filler. As calculated, the content of TaC in the C/SiC–ZrB_2–TaC composites is only 2.4 vol.%. In the TaC-lean area, ZrB_2 is oxidized according to reaction (4). The ZrO_2 can protect the fiber from being ablated. However, ZrO_2 with a loose structure can be removed by the high flux rate, and the fiber becomes uncovered. In the TaC-rich area, TaC will be oxidized to generate a large amount of liquid Ta_2O_5 when the ablation temperature is higher than 1870 °C (reaction (5)). The Ta_2O_5 liquid phase can not only seal the cracks during ablation but also hold the loose ZrO_2 to form a dense layer around the fibers. The fibers are thus protected. In order to further improve the ablation resistance of the C/SiC–ZrB_2–TaC composites, the content of TaC should be increased, and its distribution in the matrix should be improved.

4. Conclusion

2D C/SiC–ZrB_2–TaC composites were fabricated by CVI combined with SP method. Properties including flexural strength, interlaminar shear strength, and CTE of the composites were investigated. The ablation test was carried out under an oxyacetylene torch flame. The morphologies of the ablated specimens were analyzed. The results indicate that the

addition of vertical fiber tows into the laminate and the heat-treatment at 1800 °C greatly increase the interlaminar shear strength. The co-addition of ZrB_2 and TaC powders into C/SiC composite can enhance its ablation resistance.

Acknowledgements

This work is financially supported by the Chinese Natural Science Foundation (Grant # 90716023) and by the Research Fund of State Key Laboratory of Solidification Processing (NWPU), China (Grant # 21-TP2007).

References

[1] N.S. Jacobson, Corrosion of silicon-based ceramics in combustion environments, J. Am. Ceram. Soc. 76 (1993) 3–28.
[2] Y. Wang, L. An, Y. Fan, L. Zhang, S. Burton, Z. Gan, Oxidation of polymer-derived SiAlCN ceramics, J. Am. Ceram. Soc. 88 (2005) 3075–3080.
[3] S. Schmidt, S. Beyer, H. Knabe, H. Immich, R. Meistring, A. Gessler, Advanced ceramic matrix composite materials for current and future propulsion technology applications, Acta Astronaut. 55 (2004) 409–420.
[4] W. Krenkel, F. Berndt, C/C–SiC composites for space applications and advanced friction systems, Mater. Sci. Eng. A 412 (2005) 177–181.
[5] K. Upadhya, J.M. Yang, W.P. Hoffman, Materials for ultrahigh temperature structural applications, J. Am. Ceram. Soc. 12 (1997) 51–56.
[6] F. Christin, Design, fabrication, and application of thermostructural composites (TSC) like C/C, C/SiC, and SiC/SiC composites, Adv. Eng. Mater. 4 (2002) 903–912.
[7] W.G. Fahrenholtz, G.E. Hilmas, UHTM Workshop Draft Report NSF-AFOSR Joint Workshop on Future Ultra-High Temperature Materials, 2004.
[8] Y. Wang, Y.D. Xu, Y.G. Wang, L.F. Cheng, L.T. Zhang, Effects of TaC addition on the ablation resistance of C/SiC, Mater. Lett. 64 (2010) 2068–2071.
[9] Y.G. Wang, Q.M. Liu, J.L. Liu, L.T. Zhang, L.F. Cheng, Deposition mechanism for chemical vapor deposition of zirconium carbide coatings, J. Am. Ceram. Soc. 91 (2008) 1249–1252.
[10] H.B. Li, L.T. Zhang, L.F. Cheng, Y.G. Wang, Ablation resistance of different coating structures for C/ZrB2–SiC composites under oxyacetylene torch flame, Int. J. Appl. Ceram. Technol. 6 (2009) 145–150.
[11] A. Sayir, Carbon fiber reinforced hafnium carbide composite, J. Mater. Sci. 39 (2004) 5995–6003.
[12] S.F. Tang, J.Y. Deng, S.J. Wang, W.C. Liu, Fabrication and characterization of an ultra-high-temperature carbon-fiber reinforced ZrB_2–SiC matrix composites, J. Am. Ceram. Soc. 90 (2007) 3320–3322.
[13] W.H. Glime, J.D. Cawley, Oxidation of carbon fibers and films in ceramic matrix composites: a weak link process, Carbon 33 (1995) 1053–1060.
[14] C.R. Wang, J.M. Yang, W. Hoffman, Thermal stability of refractory carbide/boride composites, Mater. Chem. Phys. 74 (2002) 272–281.
[15] S. Rangarajan, R. Belardinelli, P.B. Aswath, Processing, physical and thermal properties of Blackglas™ matrix composites reinforced with Nextel™ fabric, J. Mater. Sci. 34 (1999) 515–533.
[16] R. Teghil, A. De Bonis, A. Galasso, P. Villani, A. Santagata, Femtosecond pulsed laser ablation deposition of tantalum carbide, Appl. Surf. Sci. 254 (2007) 1220–1223.
[17] W.G. Fahrenholtz, G.E. Hilmas, Refractory diborides of zirconium and hafnium, J. Am. Ceram. Soc. 90 (2007) 1347–1364.
[18] Y.G. Wang, W. Liu, L.F. Cheng, L.T. Zhang, Preparation and properties of 2D C/ZrB_2–SiC ultra high temperature ceramic composites, Mater. Sci. Eng. A 524 (2009) 129–133.
[19] S. Singh, V.K. Srivastava, Effect of oxidation on elastic modulus of C/C–SiC composites, Mater. Sci. Eng. A 486 (2008) 534–539.
[20] H.B. Li, L.T. Zhang, L.F. Cheng, Y.G. Wang, Z.J. Yu, M. Huang, H.B. Tu, H.P. Xia, Polymer–ceramic conversion of a highly branched liquid polycarbosilane for SiC-based ceramics, J. Mater. Sci. 43 (2008) 2806–2811.
[21] M. Zhu, Y.G. Wang, Pressureless sintering ZrB_2–SiC ceramics at low temperatures, Mater. Lett. 63 (2009) 2035–2037.
[22] Q. Zhang, L.F. Cheng, L.T. Zhang, Y.D. Xu, Thermal expansion behavior of carbon fiber reinforced chemical-vapor-infiltrated silicon carbide composites from room temperature to 1400 °C, Mater. Lett. 60 (2006) 3245–3247.
[23] R.Y. Luo, T. Liu, J.S. Li, H.B. Zhang, Z.J. Chen, G.L. Tian, Thermophysical properties of carbon/carbon composites and physical mechanism of thermal expansion and thermal conductivity, Carbon 42 (2004) 2887–2895.
[24] W.D. Fei, L.D. Wang, Thermal expansion behavior and thermal mismatch stress of aluminum matrix composite reinforced by β-eucryptite particle and aluminum borate whisker, Chem. Phys. 85 (2004) 450–457.